AIAA JOURNAL
Vol. 33, No. 6, June 1995

Interaction of a Weak Shock with Freestream Disturbances

Zvi Rusak,* Thomas E. Giddings,† and Julian D. Cole‡
Rensselaer Polytechnic Institute, Troy, New York 12180-3590

A new transonic small-disturbance model to analyze the interactions of freestream disturbances with a weak shock has been developed. The model equation has an extended form of the classic small-disturbance equation for unsteady transonic aerodynamics. An alternative approach shows that the pressure field may be described by an equation that has an extended form of the classic nonlinear acoustic equation that describes the propagation of sound beams with a narrow angular spectrum. The model shows that diffraction effects, nonlinear steepening effects, focusing effects, and induced vorticity fluctuations interact simultaneously to determine the development of the shock wave in space and time and the pressure field behind it. A finite difference algorithm to solve the mixed-type elliptic/hyperbolic flows around the shock wave has also been developed. Numerical calculations of shock wave interactions with various deterministic vorticity and temperature disturbances result in complicated shock wave structures and describe peaked as well as rounded pressure signatures across the shock front, as were recorded in experiments of sonic booms running through atmospheric turbulence.

Nomenclature

c	= speed of sound
F, G	= arbitrary functions, Eqs. (7)
f, g	= freestream perturbation functions, Eqs. (18)
h, h_1	= shock front shape in nonlinear and linear analyses, respectively
$\boldsymbol{i}, \boldsymbol{j}, \boldsymbol{k}$	= unit vectors in x, y, z directions
i, j, k, n	= indices of a point in the numerical mesh
K	= similarity parameter, $(M_\infty^2 - 1)/\epsilon^{\frac{2}{3}}$
M	= Mach number
P	= pressure in nonlinear analysis
p	= nondimensional pressure perturbation
S	= entropy
s	= nondimensional entropy perturbation
T	= nondimensional temperature perturbation
T_m	= temperature
t	= time
t^*	= rescaled time
U	= uniform speed
u, u_1, u_2	= axial velocity perturbations, x direction
$\boldsymbol{V}$	= velocity vector
v, v_1, v_2	= velocity perturbations in y direction
w, w_1, w_2	= velocity perturbations in z direction
x, y, z	= coordinates
x^*	= rescaled x coordinate
γ	= ratio of specific heats, 1.4 for air
$\Delta( )$	= difference of a quantity
ϵ	= small quantity, $\ll 1$
ξ_j	= modified axial coordinate, $x - U_{0j}t$
$\boldsymbol{v}_{1j}$	= perturbed velocity vector
$\rho, \bar{\rho}$	= density
ρ_{sj}	= arbitrary function, Eqs. (7)
τ_j	= modified time, $U_{0j}t$
ϕ	= potential
ω	= vorticity vector

Subscripts

a	= ahead of the shock front
b	= behind the shock front
j	= index, a or b
$j0, j\omega$	= of irrotation and rotational solutions, respectively
$0, 0_j$	= basic state property
1	= perturbed quantity
∞	= freestream conditions
$*$	= scaled perturbation, Eq. (21)

Superscripts

$*$	= scaled quantity, Eq. (19)
b	= backward differencing
c	= centered differencing
$\tilde{}$	= nondimensional functions, Eqs. (10)

Received June 4, 1994; revision received Jan. 4, 1995; accepted for publication Jan. 5, 1995.

*Assistant Professor, Department of Mechanical Engineering, Aeronautical Engineering and Mechanics. Senior Member AIAA.

†Graduate Student, Department of Mechanical Engineering, Aeronautical Engineering and Mechanics. Student Member AIAA.

‡Margaret Darrin Distinguished Professor of Applied Mathematics, Department of Mathematical Sciences. Fellow AIAA.

I. Introduction

EXPERIMENTAL data exist showing the pressure profiles of sonic booms, created by the passage of a distant supersonic aircraft, can be drastically affected by freestream atmospheric turbulence.[1-5] The usual N wave or a shaped sonic boom profile can randomly exhibit either large-pressure peaks with short rise times, rounded profiles with longer rise times, or messy pressure signatures. Recent laboratory model experiments of turbulence affect on the rise time and waveform of N waves have shown similar results.[6] The interaction of the sonic boom with the atmospheric turbulence, specifically in the atmospheric boundary layer near the ground, may result in higher and unacceptable loudness levels.[7] Therefore, in order to get reasonable estimates of the sonic boom performance of various designs of a future supersonic transport airplane, it is essential to understand the basic interactions of the atmospheric turbulence with weak shock waves.

The basic analysis of the distortion of sonic bangs by atmospheric turbulence was given by Crow.[8] Using a first-order acoustic scattering theory, Crow showed that the pressure perturbation behind the shock is related to the interaction of the shock with the disturbances it encounters while moving in the atmosphere. The pressure profile can be calculated by a surface integral over a paraboloid of dependence, whose focus is the observation point and whose directrix is the shock front. By describing the turbulent eddies in the Kolmogorov inertial subrange, it was found that the mean-square pressure perturbation behind the shock changes like $(\Delta p)^2(t_c/t)^{7/6}$ where (Δp) is the pressure jump across the shock, (t) is time after the shock passes an observation point, and (t_c) is a critical time predicted in terms of meteorological conditions. Crow's analysis[8] predicts reasonable average values of the pressure fluctuations for times (t) comparable to (t_c).

The singularity in the pressure perturbations near the shock front (when $t \to 0$) was analyzed by Plotkin and George.[9] A second-

order acoustic scattering theory was used to describe rounded shock signatures. The average of the diffraction effects was approximated as a dissipation term. The thickening of the shock is explained as a balance between nonlinear steepening effects and the dissipative effect of the turbulent scattering of acoustic energy out of the incident shock. Rise time predictions of this theory show some correlation with experimental data. On the other hand, Ffowcs Williams and Howe[10] examined the approaches that describe the possibility of a turbulent thickening of weak shock waves and reached a conclusion that atmospheric turbulence cannot be the cause of shock thickening. They suggested that weak shocks may attain a dispersed profile due to nonequilibrium gas effects.

It should be emphasized that the scattering analyses of Refs. 8–10 considered weak turbulent perturbations relative to the shock strength, whereas in the case of the sonic boom interaction with atmospheric turbulence the random flow fluctuations may be of the same order of the shock wave strength and may strongly distort the shock front. In addition, these analyses did not account for shock jump conditions that must be satisfied in an inviscid analysis across any shock surface. The approximation made in Ref. 9 of the average diffraction effects described as a dissipative term may also be questioned.

A different approach was taken by Pierce.[11,12] He interpreted the spikes observed on sonic boom pressure waveforms as being due to the simultaneous focusing and diffraction of a nearly planar *N* wave by an inhomogeneous layer in the atmosphere. The shock front develops ripples that are transformed into folds in the front when the shock passes vertices of caustics. This mechanism results in a fine structure of very small pressure jumps that correspond to the various segments of the folded wave front. Pierce[12] derived a stochastic model of a shock front propagating through a turbulent atmosphere to substantiate the very small discrete structure of sonic boom profiles.

Pierce's model,[11,12] however, neglects nonlinear effects that become significant, specifically near a caustic vertex, as was shown by Cramer and Seebass[13] and Gill and Seebass.[14] Cramer and Seebass[13] described the focusing of a very weak and slightly concave shock wave by the unsteady transonic small-disturbance flow equation. Gill and Seebass[14] derived an approximate analytical solution of the steady transonic small-disturbance problem for the nonlinear behavior of a weak compression wave with a finite rise time near a caustic. They calculated the reflected shock wave from a caustic and provided an estimate of its strength. The experimental results of Sturtevant and Kulkarny[15] also show that focusing effects are significant for weak shock waves as occurs in the case of the sonic boom signatures.

Sparrow and Pierce[16] have recently presented a simple statistical prediction for how often sonic booms propagating in the Earth's boundary layer will encounter caustics. The theory is based on describing the variation of ray tube areas of a sound wave propagating in a turbulent medium by a generic harmonic oscillator equation. For measured realizations of atmospheric turbulence the model predicts that sonic booms will exhibit spikes with the occurrence of caustics after propagating a very short distance in the random medium, thus agreeing with the predictions of Pierce.[11,12]

In a recent paper, Pierce[17] has derived a model equation to describe the development of sonic boom signatures in atmospheric turbulence. The equation has been constructed by using physical considerations only. It extends geometrical acoustic approximations to include convection at the wave speed, diffraction effects, molecular relaxation, classical dissipation, and nonlinear steepening effects. The atmospheric turbulence enters through an effective speed of sound which varies randomly in time and space. However, since this theory has not been developed consistently from the fluid dynamic equations, Pierce[17] raised questions whether all of the effects are necessary in his suggested model and how to accomplish a numerical or analytical solution to the problem.

Related to the problem of the sonic boom interaction with turbulence is the basic question of the interaction of a shock wave with a vortical flow and, specifically, with a vortex or a train of eddies.[18–21] The research of the latter problem was basically motivated by the interest to reduce the noise and vibrations produced by high-speed supersonic vehicles. For these problems, the interaction of relatively strong shock waves with turbulent jets or wakes is a significant source of noise. The shock-vortex system is a basic element of these more complex interactions.[21] It can also shed light on the sonic boom interaction with atmospheric turbulence, specifically, when the shocks are weak and vortex strength is comparable to the shock strength.

Experimental results of shock-vortex systems[18–21] revealed curved, diffracted shocks as well as complicate structures of curved, reflected shock waves from the incident shock front due to the vortex induced flowfield. The pressure field behind the shock contains regions of compressions and rarefactions that produce acoustic waves. Similar shock structures were also observed by Sturtevant and Kulkarny[15] who investigated the focusing of weak, curved shock waves. Of specific interest are measurements of Dosanjh and Weeks[19] of the shock wave interaction with a vortex street. The shock front is distorted by the wake flow which results in a focusing process, whereas the vortex street is dissolved by the shock.

The analyses of the shock-vortical flow interactions are limited to linear perturbation theories only.[22–26] These analyses considered the jump conditions across a shock surface and predicted the development of vorticity waves, entropy waves, and acoustic waves behind the shock front.[22–24] The acoustic wave was approximated by a quadrupole[26] or as a sum of monopole, dipole, and quadrupole acoustic sources. Recent direct numerical simulations of isotropic turbulence interacting with a weak shock by Lee et al.[27] show good correlation with the linear analysis predictions of Ribner[24] for weak disturbances. However, since all of these theories are linear, they cannot account for any nonlinear effects, such as large shock distortions, focusing, and nonlinear steepening effects that are usually found in experiments[15,18,19] or in numerical simulations of shock-vortex interactions.[28–30]

The review of experimental and theoretical investigations of the interaction of shock waves with freestream vortical or turbulent flows shows that this complex nonlinear interaction is still an open problem. Specifically, the improved simulation of sonic boom propagation through the real atmosphere requires a better understanding of the interaction of weak shocks with vortical perturbations and turbulence.[16]

Analysis of the experimental data and the theoretical approaches shows that in the case of the sonic boom, the shock waves near the ground are very weak but still stronger than any acoustic wave. Also, flow fluctuations due to the atmospheric turbulence or vortical shear flows can become comparable to the shock wave strength such that locally the shock strength can be either strongly reduced or magnified and the shock wave front can be distorted significantly. Therefore, linearized acoustics and its second-order scattering problem, or first-order linear theories of shock-vorticity interaction do not correctly represent the development of the shock front and the pressure field behind it (see also Sec. II). However, in a coordinate system moving with the basic weak shock, the problem may fit the transonic framework.[31]

This paper presents a new extended transonic small-disturbance model that has been developed to describe the interactions of freestream fluctuations with a weak shock wave. The model equations also has an extended form of the classic nonlinear acoustics equation that describes the propagation of sound beams with narrow angular spectrum (KKZ equation).[32,33] The model shows that diffraction effects, nonlinear steepening, focusing, and induced freestream disturbances interact simultaneously to determine the development of the shock wave and the pressure field behind it. A finite difference algorithm to solve the mixed-type elliptic/hyperbolic flows around the shock wave is also presented. Numerical calculations of weak shock wave interactions with deterministic fluctuations describe both peaked or rounded pressure signatures as were recorded in experiments of sonic booms running through atmospheric turbulence.

II. Breakdown of the Linearized Theory

A. Linearized Theory

An inviscid and nonheat conducting flow is assumed. A normal shock with a uniform supersonic oncoming stream and a uniform subsonic outgoing flow is considered. The upstream flow ahead of the shock is characterized by a speed U_{0a} in the x direction, pressure p_{0a}, and density ρ_{0a} and the downstream flow behind the shock by U_{0b}, p_{0b}, and ρ_{0b}, respectively. Assuming the shock front is given by the $x = 0$ plane, the jump conditions across a normal shock[34] show that

$$\begin{aligned} \rho_{0a}U_{0a} &= \rho_{0b}U_{0b} \\ \rho_{0a}U_{0a}^2 + p_{0a} &= \rho_{0b}U_{0b}^2 + p_{0b} \\ \tfrac{1}{2}\rho_{0a}U_{0a}^3 + \frac{\gamma}{\gamma-1}p_{0a}U_{0a} &= \tfrac{1}{2}\rho_{0b}U_{0b}^3 + \frac{\gamma}{\gamma-1}p_{0b}U_{0b} \end{aligned} \tag{1}$$

Small disturbances are considered in each of the uniform streams. The velocity vector $\boldsymbol{V}$, pressure P, density ρ, and vorticity ω may be given ahead ($j = a$) and behind the shock ($j = b$) by

$$\begin{aligned} \boldsymbol{V}_j &= U_{0j}(\boldsymbol{i} + \epsilon \boldsymbol{v}_{1j} + \cdots) \\ P_j &= P_{0j}(1 + \epsilon p_{1j}) \\ \rho_j &= \rho_{0j}(1 + \epsilon\rho_{1j} + \cdots) \\ \omega_j &= \epsilon\omega_{1j} + \cdots, \qquad \omega_{1j} = \nabla \times \boldsymbol{v}_{1j} \end{aligned} \tag{2}$$

Here $\boldsymbol{v}_{1j}$, p_{1j}, and ρ_{1j} are functions of (x, y, z, t). An axial coordinate moving with the uniform speed is considered in each region, $\xi_j = x - U_{0j}t$, $\tau_j = U_{0j}t$. The substitution into the continuity, momentum, and energy equations results to the leading order in $[\nabla = (\partial/\partial\xi_j)\boldsymbol{i} + (\partial/\partial y)\boldsymbol{j} + (\partial/\partial z)\boldsymbol{k}]$

$$\begin{aligned} \frac{\partial\rho_{1j}}{\partial\tau_j} + \nabla\cdot\boldsymbol{v}_{1j} &= 0 \\ \frac{\partial\boldsymbol{v}_{1j}}{\partial\tau_j} + \frac{1}{\gamma M_{0j}^2}\nabla p_{1j} &= 0 \\ \frac{\partial p_{1j}}{\partial\tau_j} + \gamma(\nabla\cdot\boldsymbol{v}_{1j}) &= 0 \end{aligned} \tag{3}$$

Equations (3) result in

$$\frac{\partial p_{1j}}{\partial\tau_j} = \gamma\frac{\partial\rho_{1j}}{\partial\tau_j}, \qquad \frac{\partial\omega_{1j}}{\partial\tau_j} = 0, \qquad M_{0j}^2\frac{\partial^2 p_{1j}}{\partial\tau_j^2} - \nabla^2 p_{1j} = 0 \tag{4}$$

where $M_{0j} = U_{0j}/c_{0j}$ and $c_{0j}^2 = \gamma p_{0j}/\rho_{0j}$. Equations (4) show that $\omega_{1j} = \omega_{1j}(\xi_j, y, z)$ and that the pressure perturbation p_{1j} is described by the acoustic equation. Therefore, the first-order disturbance flow can be split into a linear combination of rotational and irrotational parts: $\boldsymbol{v}_{1j} = \boldsymbol{v}_{1j\omega} + \boldsymbol{v}_{1j0}$. The rotational part may be described essentially by incompressible flow equations

$$\nabla\cdot\boldsymbol{v}_{1j\omega} = 0, \qquad \nabla\times\boldsymbol{v}_{1j\omega} = \omega_{1j}(\xi_j, y, z) \tag{5a}$$

The irrotational (potential) part may be described by acoustics equations relative to the basic flow in each region

$$\begin{aligned} \boldsymbol{v}_{1j0} &= \nabla\phi_j, \qquad p_{1j} = -\gamma M_{0j}^2\frac{\partial\phi_j}{\partial\tau_j}, \\ M_{0j}^2\frac{\partial^2\phi_j}{\partial\tau_j^2} &- \nabla^2\phi_j = 0 \end{aligned} \tag{5b}$$

The first-order perturbation theory also considers the distortion of the shock front. Assuming that the perturbed shock front is given by $x - \epsilon h_1(y, z, t) = 0$, the exact jump conditions across the shock[34] result to the leading order in a set of conditions that must be satisfied along the $x = 0$ plane for any (y, z, t),

$$\rho_{1a}(0, y, z, t) + u_{1a}(0, y, z, t) - (h_{1t}/U_{0a}) = \rho_{1b}(0, y, z, t) + u_{1b}(0, y, z, t) - (h_{1t}/U_{0b}) \tag{6a}$$

$$U_{0a}\left[\rho_{1a}(0, y, z, t) + 2u_{1a}(0, y, z, t) + \left(1/\left(\gamma M_{0a}^2\right)\right)p_{1a}(0, y, z, t)\right] = U_{0b}\left[\rho_{1b}(0, y, z, t) + 2u_{1b}(0, y, z, t) + \left(1/\left(\gamma M_{0b}^2\right)\right)p_{1b}(0, y, z, t)\right] \tag{6b}$$

$$\begin{aligned} U_{0a}^2\Bigg\{&\rho_{1a}(0, y, z, t) + 3u_{1a}(0, y, z, t) \\ &+ \frac{2}{(\gamma-1)M_{0a}^2}[p_{1a}(0, y, z, t) + u_{1a}(0, y, z, t)] \\ &- \frac{h_{1t}}{U_{0a}}\left[1 + \frac{2}{(\gamma-1)\gamma M_{0a}^2}\right]\Bigg\} \\ = U_{0b}^2\Bigg\{&\rho_{1b}(0, y, z, t) + 3u_{1b}(0, y, z, t) \\ &+ \frac{2}{(\gamma-1)M_{0b}^2}[p_{1b}(0, y, z, t) + u_{1b}(0, y, z, t)] \\ &- \frac{h_{1t}}{U_{0b}}\left[1 + \frac{2}{(\gamma-1)\gamma M_{0b}^2}\right]\Bigg\} \end{aligned} \tag{6c}$$

$$U_{0a}[v_{1a}(0, y, z, t) + h_{1y}] = U_{0b}[v_{1b}(0, y, z, t) + h_{1y}] \tag{6d}$$

$$U_{0a}[w_{1a}(0, y, z, t) + h_{1z}] = U_{0b}[w_{1b}(0, y, z, t) + h_{1z}] \tag{6e}$$

Here $h_{1t} = \partial h_1/\partial t$, $h_{1y} = \partial h_1/\partial y$, $h_{1z} = \partial h_1/\partial z$ and (u_{1j}, v_{1j}, w_{1j}) are the components of the velocity perturbation $\boldsymbol{v}_{1j}$. The linearized jump conditions in Eqs. (6) include the entropy increase produced by the shock. It can be shown from Eqs. (5) and (6) that (using the solution of the downstream equations for the disturbance flow) the shock conditions are adequate to describe the flow downstream of the shock wave and its distorted motion for given upstream disturbances.

B. One-Dimensional Flow

In the case of a one-dimensional flow, the rotational part vanishes identically, and the solution of the acoustic equation ahead ($j = a$) and behind ($j = b$) the shock is given by

$$\begin{aligned} u_{1j} &= F\left(\xi_j - \frac{\tau_j}{M_{0j}}\right) + G\left(\xi_j + \frac{\tau_j}{M_{0j}}\right) \\ p_{1j} &= \gamma M_{0j}\left[F\left(\xi_j - \frac{\tau_j}{M_{0j}}\right) - G\left(\xi_j + \frac{\tau_j}{M_{0j}}\right)\right] \\ \rho_{1j} &= M_{0j}\left[F\left(\xi_j - \frac{\tau_j}{M_{0j}}\right) - G\left(\xi_j + \frac{\tau_j}{M_{0j}}\right) + \rho_{sj}(\xi_j)\right] \end{aligned} \tag{7}$$

where F and G are arbitrary functions that describe the upstream and downstream acoustic waves. Here ρ_{sj} is an arbitrary function that describes entropy waves that are convected with the flows [the first-order entropy disturbance is given by $S_j - S_{0j} = \epsilon s_{1j} = \epsilon c_p M_{0j}\rho_{sj}(\xi_j)$, where S_j is the entropy in region j, $S_{0j} = c_v \ln(P_{0j}/\rho_{0j}^{\gamma})$ and c_v and c_p are the specific heat constants]. Assuming that no acoustic waves can propagate upstream, specifically not in the flow behind the shock, then $G \equiv 0$. Then the shock jump conditions (6) provide a system of three linear equations for the solution of the downstream acoustic and entropy waves $F_b(\xi_b - \tau_b/M_{0b})$ and

$\rho_{sb}(\xi_b)$ and the shock position rate of change in time $h_{1t}(t)$ in terms of the given acoustic and entropy perturbations $F_a(\xi_a - \tau_a/M_{0a})$ and $\rho_{sa}(\xi_a)$ in the upstream flow. Let

$$\begin{aligned} F_{a0} &= F_a[-(U_{0a}+c_{0a})t], \qquad \rho_{sa0} = \rho_{sa}(-U_{0a}t) \\ F_{b0} &= F_b[-(U_{0b}+c_{0b})t], \qquad \rho_{sb0} = \rho_{sb}(-U_{0b}t) \end{aligned} \tag{8}$$

Then from Eqs. (6–8), we get

$$(1+M_{0b})F_{b0} + M_{0b}\rho_{sb0} + \left[\frac{U_{0b}}{U_{0a}} - 1\right]\frac{h_{1t}}{U_{0b}} = (1+M_{0a})F_{a0} + M_{0a}\rho_{sa0} \tag{9a}$$

$$\left[2 + M_{0b} + \frac{1}{M_{0b}}\right]F_{b0} + M_{0b}\rho_{sb0} = \frac{U_{0a}}{U_{0b}}\left[\left(2 + M_{0a} + \frac{1}{M_{0a}}\right)F_{a0} + M_{0a}\rho_{sa0}\right] \tag{9b}$$

$$\left[3 + M_{0b} + \frac{2}{(\gamma-1)M_{0b}^2}(1+\gamma M_{0b})\right]F_{b0} + M_{0b}\rho_{sb0} + \left\{\frac{U_{0a}}{U_{0b}}\left[1 + \frac{2/\gamma}{(\gamma-1)M_{0a}^2}\right] - 1 - \frac{2/\gamma}{(\gamma-1)M_{0b}^2}\right\}\frac{h_{1t}}{U_{0b}} = \frac{U_{0a}^2}{U_{0b}^2}\left\{\left[3 + M_{0a} + \frac{2}{(\gamma-1)M_{0a}^2}(1+\gamma M_{0a})\right]F_{a0} + M_{0a}\rho_{sa0}\right\} \tag{9c}$$

The determinant of the system (9) may be written in the form $\Delta = (M_{0a}^2 - 1)\mathrm{fn}(M_{0a}^2)$. Therefore, the solution of Eqs. (9) shows that the shock front motion and the perturbed flow behind it may be described by

$$\begin{aligned} x &= \frac{\epsilon}{M_{0a}^2 - 1}\tilde{h}_1(t; M_{0a}) \\ u_{1b} &= U_{0b}\left[1 + \frac{\epsilon}{M_{0a}^2-1}\tilde{u}_1(x,t;M_{0a}) + \cdots\right] \\ p_{1b} &= P_{0b}\left[1 + \frac{\epsilon}{M_{0a}^2-1}\tilde{p}_1(x,t;M_{0a}) + \cdots\right] \\ \rho_{1b} &= \rho_{0b}\left[1 + \frac{\epsilon}{M_{0a}^2-1}\tilde{\rho}_1(x,t;M_{0a}) + \cdots\right] \end{aligned} \tag{10}$$

where functions $\tilde{h}_1$, $\tilde{u}_1$, $\tilde{p}_1$, and $\tilde{\rho}_1$ can be expressed in terms of the given flow perturbations ahead of the shock wave. In principle, these expressions may enable spectral characterization of the pressure fluctuations and the turbulence downstream of the shock wave in terms of the spectral characterization of the incoming turbulence. However, Eqs. (10) show that the linear approach is nonuniform when the shock wave is very weak $M_{0a}^2 \to 1^+$ and also when the flow fluctuations are of the same order of the shock strength, $\epsilon \sim (M_{0a}^2 - 1)$, as in the case of the interaction of the sonic boom with atmospheric turbulence. A similar nonuniformity is also found from the analysis of two- or three-dimensional flows. This uniformity problem leads to a different approach to study the interaction of a weak shock with comparable random fluctuations in the flow.

III. Transonic Small Disturbance Model

The analysis of the linearized problem of the interaction of a weak shock with small disturbances shows that it is an invalid approach when the flow perturbations are of the order of the shock strength. Therefore, a different approach has been developed to study the interaction of weak shocks with comparable random fluctuations in the flow. In a coordinate system moving with a basic given weak shock, the problem may fit the framework of transonic theory.[31] A transonic small-disturbance model is developed to analyze the flow across a basic weak shock running in the $-x$ direction. A coordinate system attached to the basic shock is considered. The transonic regime is characterized by perturbations in the velocity component normal to the shock that are much larger than the transverse velocity components. Therefore, the velocity vector V, pressure P, density $\bar{\rho}$, and vorticity ω may be described everywhere in the flow by

$$\begin{aligned} \boldsymbol{V} &= U_\infty\left\{\boldsymbol{i}\left(1 + \epsilon^{\frac{2}{3}}u + \epsilon u_1 + \epsilon^{\frac{4}{3}}u_2 + \cdots\right)\right. \\ &\quad \left. + \boldsymbol{j}\left(\epsilon v_1 + \epsilon^{\frac{4}{3}}v_2 + \cdots\right) + \boldsymbol{k}\left(\epsilon w_1 + \epsilon^{\frac{4}{3}}w_2 + \cdots\right)\right\} \\ P &= p_\infty\left(1 + \epsilon^{\frac{2}{3}}p + \epsilon p_1 + \epsilon^{\frac{4}{3}}p_2 + \cdots\right) \\ \bar{\rho} &= \rho_\infty\left(1 + \epsilon^{\frac{2}{3}}\rho + \epsilon\rho_1 + \epsilon^{\frac{4}{3}}\rho_2 + \cdots\right) \\ \omega &= \epsilon^{\frac{2}{3}}(\boldsymbol{j}\omega_y + \boldsymbol{k}\omega_z) + \epsilon(\boldsymbol{i}\omega_{x1} + \boldsymbol{j}\omega_{y1} + \boldsymbol{k}\omega_{z1}) + \cdots \end{aligned} \tag{11}$$

Here $M_\infty^2 \equiv U_\infty^2/c_\infty^2 = 1 + K\epsilon^{\frac{2}{3}}$ is the Mach number of the undisturbed moving shock ($K > 0$) and c_∞, p_∞ and ρ_∞ are the speed of sound, pressure, and density of the unperturbed flow ahead of the shock. The symbol $(\epsilon^{\frac{2}{3}})$, represents the scale of strength of the basic weak shock where $\epsilon \ll 1$. K is a similarity parameter that indicates the ratio of shock strength to freestream disturbances. Also, the constant K reflects that the speed of the basic shock wave is slightly higher than the speed of sound ahead of the shock. A rescaling of the x coordinate and time t has also been considered: $x^* = x/\epsilon^{\frac{1}{3}}$ and $t^* = tc_\infty\epsilon^{\frac{1}{3}}$, such that each of the terms in Eqs. (11) is a function of (x^*, y, z, t^*). The rescaling in the x direction leads to a stretching of the picture of the flow around the basic shock in order to capture the nonlinear interactions that occur in the flow across the shock. The rescaling in time accounts for low-frequency, unsteady perturbations in the flow. The substitution of Eqs. (11) into the continuity, momentum, and energy equations results to the leading orders in

$$\begin{cases} \dfrac{\partial}{\partial x^*}(\rho + u) = 0 \\ \dfrac{\partial}{\partial x^*}(\rho_1 + u_1) = 0 \\ \dfrac{\partial \rho}{\partial t^*} + \dfrac{\partial}{\partial x^*}(u_2 + \rho_2 + \rho u) + \dfrac{\partial v_1}{\partial y} + \dfrac{\partial w_1}{\partial z} = 0 \end{cases} \tag{12}$$

$$\begin{cases} \dfrac{\partial}{\partial x^*}(\gamma u + p) = 0 \\ \dfrac{\partial}{\partial x^*}(\gamma u_1 + p_1) = 0 \\ \dfrac{\partial u}{\partial t^*} + \dfrac{\partial u_2}{\partial x^*} + (u + \rho + K) + \dfrac{\partial u}{\partial x^*} + \dfrac{1}{\gamma}\dfrac{\partial p_2}{\partial x^*} = 0 \end{cases} \tag{13}$$

$$\begin{cases} \dfrac{\partial v_1}{\partial x^*} = -\dfrac{1}{\gamma}\dfrac{\partial p}{\partial y} \\ \dfrac{\partial w_1}{\partial x^*} = -\dfrac{1}{\gamma}\dfrac{\partial p}{\partial z} \end{cases} \tag{14}$$

$$\frac{\partial p}{\partial t^*} - \gamma\frac{\partial \rho}{\partial t^*} + \rho\frac{\partial p}{\partial x^*} - \gamma p\frac{\partial \rho}{\partial x^*} + \frac{\partial p_2}{\partial x^*} - \gamma\frac{\partial \rho_2}{\partial x^*} = 0 \tag{15}$$

$$\frac{\partial \omega_y}{\partial x^*} = 0, \qquad \frac{\partial \omega_z}{\partial x^*} = 0 \tag{16}$$

From the equation of state and the definition of entropy, it can be shown that the temperature T_m and entropy S are given by

$$\begin{aligned} T_m &= T_\infty\left(1 + \epsilon^{\frac{2}{3}}T + \cdots\right) \\ S &= S_\infty\left(1 + \epsilon^{\frac{2}{3}}s + \cdots\right) \end{aligned} \tag{17a}$$

where

$$\begin{aligned} T_\infty &= p_\infty/R\rho_\infty, \qquad S_\infty = c_v\ell n\left[p_\infty/\rho_\infty^\gamma\right] \\ T &= p - \rho, \qquad s = c_v/S_\infty(p - \gamma\rho) \end{aligned} \tag{17b}$$

Equations (12–17) result in

$$u + \rho = f(y, z, t^*) \tag{18a}$$

$$\gamma u + p = g(y, z, t^*) \tag{18b}$$

$$-2\frac{\partial u}{\partial t^*} + [-K - f + g - (\gamma + 1)u]\frac{\partial u}{\partial x^*} + \frac{\partial v_1}{\partial y} + \frac{\partial w_1}{\partial z} = -\frac{1}{\gamma}\frac{\partial g}{\partial t^*} \tag{18c}$$

$$\omega_y = \frac{\partial u}{\partial z} - \frac{\partial w_1}{\partial x^*} = \frac{1}{\gamma}\frac{\partial g}{\partial z} \tag{18d}$$

$$-\omega_z = \frac{\partial u}{\partial y} - \frac{\partial v_1}{\partial x^*} = \frac{1}{\gamma}\frac{\partial g}{\partial y} \tag{18e}$$

$$T = g - f - (\gamma - 1)u, \qquad s = (c_v/S_\infty)(g - \gamma f) \tag{18f}$$

where f and g are random induced fluctuations due to the free turbulence. The function g is related to the vorticity fluctuations in the flow and the function f is due to temperature or speed of sound fluctuations. Equations (18) show that the axial perturbation u, pressure perturbation p, and density perturbation ρ, that are of the order of the shock strength $\epsilon^{\frac{2}{3}}$, interact with the transverse velocity perturbations v_1 and w_1, that are of a smaller scale ϵ.

The substitution of $u = g/\gamma + u_*$ in Eqs. (18c–18e) results in a problem for a velocity potential function $\phi(x^*, y, z, t^*)$ where

$$u_* = \frac{\partial \phi}{\partial x^*}, \quad v_1 = \frac{\partial \phi}{\partial y}, \quad w_1 = \frac{\partial \phi}{\partial z}, \quad p = -\gamma\frac{\partial \phi}{\partial x^*} \tag{19a}$$

$$2\phi_{x^*t^*} + \left[K + \frac{g}{\gamma} + f + (\gamma + 1)\phi_{x^*}\right]\phi_{x^*x^*} - (\phi_{yy} + \phi_{zz}) = -\frac{1}{\gamma}\frac{\partial g}{\partial t^*} \tag{19b}$$

In a conservative form Eq. (19b) is given by

$$\left[2\phi_{x^*} + \frac{1}{\gamma}g\right]_{t^*} + \left[\left(K + \frac{g}{\gamma} + f\right)\phi_{x^*} + (\gamma + 1)\phi_{x^*}^2/2\right]_{x^*} - (\phi_y)_y - (\phi_z)_z = 0 \tag{19c}$$

The exact shock jump conditions[34] must be satisfied along any shock surface $x^* - h(y, z, t^*) = 0$ that may appear in the solution. To the leading orders, these conditions are

$$[f] = 0, \qquad [g] = 0 \tag{20a}$$

$$-2[\phi_{x^*}]\frac{\partial h}{\partial t^*} + \left(K + \frac{g}{\gamma} + f\right)[\phi_{x^*}] + (\gamma + 1)\left[\frac{\phi_{x^*}^2}{2}\right] + [\phi_y]\frac{\partial h}{\partial y} + [\phi_z]\frac{\partial h}{\partial z} = 0 \tag{20b}$$

$$[\phi_y] + [\phi_{x^*}]\frac{\partial h}{\partial y} = 0, \qquad [\phi_z] + [\phi_{x^*}]\frac{\partial h}{\partial z} = 0 \tag{20c}$$

where $[\varphi]$ represents the jump across the shock of property φ, $[\varphi] = \varphi_B - \varphi_A$. Equations (20a) show that to the leading order there is no jump in entropy across the shock, $[S] = 0$. Equations (11) and (18) also show that the local Mach number M_ℓ at any point in the flow is given by:

$$M_\ell^2 - 1 = \epsilon^{\frac{2}{3}}u^*, \quad u^* = \{(\gamma + 1)\phi_{x^*} + K + f + (g/\gamma)\} \tag{21}$$

The flow is locally supersonic when $(\gamma+1)\phi_{x^*}+K+f+g/\gamma > 0$, sonic when $(\gamma + 1)\phi_{x^*} + K + f + g/\gamma = 0$, and subsonic when $(\gamma + 1)\phi_{x^*} + K + f + g/\gamma < 0$. Equations (19) and (20) are an extended version of the classic unsteady small-disturbance equation for transonic aerodynamics.[31] The changes are due to the random terms g and f. Starting from given functions for f and g and initial conditions that describe a given basic shock, Eqs. (19) and (20) can be integrated in space and time to describe the development of the shock wave and pressure field behind it. A numerical algorithm to solve these equations is described in Sec. IV.

An alternative approach may be found by taking an x^* derivative of Eq. (18c) and using Eqs. (18a) and (14). The pressure perturbation p satisfies the equation

$$\frac{\partial}{\partial x^*}\left[\frac{\partial p}{\partial t^*} + \frac{K + f + g/\gamma}{2}p - \frac{\gamma + 1}{2\gamma}p\frac{\partial p}{\partial x^*}\right] = \frac{1}{2}\left[\frac{\partial^2 p}{\partial y^2} + \frac{\partial^2 p}{\partial z^2}\right] \tag{22}$$

Equation (22) is an extended version of the classic KKZ equation that describes the propagation of nonlinear sound beams with narrow angular spectrum in an inviscid fluid.[32,33] Equation (22) also has a similar form to the model equation that has been recently developed by Pierce[17] using physical considerations only.

Equations (19) and (22) show that diffraction effects, nonlinear steepening, focusing, and freestream induced fluctuations due to turbulence interact simultaneously to determine the development of the shock wave in space and time and the pressure field behind it. Disturbances tend to change the local speed of sound in the flow across the shock and through this effect to reduce or to magnify the strength of the jump along the basic shock [see Eq. (21)] or to distort the shock front. These changes may result in unsteady motion of the shock front or in caustic vertices or in reflected shocks behind the incident wave that can produce the variety of pressure signatures of sonic booms that are measured in experiments.[1–5]

IV. Finite Difference Scheme

A finite difference algorithm to solve the unsteady mixed-type elliptic/hyperbolic flow around the shock wave has been developed. Murman and Cole[35] and Cole and Cook[31] techniques are used. A fully conservative scheme that is based on the conservative form of Eq. (19c) is used. In this way the difference equations also contain the shock relations [Eqs. (20)].

Consider a uniform finite difference mesh $(\Delta x^*, \Delta y, \Delta z, \Delta t^*)$ in space and time, with points (x^*, y, z, t^*) labeled by (i, j, k, n). The results can be easily generalized to a variable mesh. Equation (19c) can be expressed in a conservative flux form for a box centered on a mesh point (i, j, k). Therefore,

$$\begin{aligned}&(1/\Delta t^*)\{(2\phi_{x^*} + g/\gamma)_{(i,j,k,n)} - (2\phi_{x^*} + g/\gamma)_{(i,j,k,n-1)}\}\\ &\quad + (1/\Delta x^*)\{\left[(K + g/\gamma + f)\phi_{x^*} + (\gamma + 1)\phi_{x^*}^2/2\right]_{(i+1/2,j,k,n)}\\ &\quad - \left[(K + g/\gamma + f)\phi_{x^*} + (\gamma + 1)\phi_{x^*}^2/2\right]_{(i-1/2,j,k,n)}\}\\ &\quad - (1/\Delta y)\{(\phi_y)_{(i,j+1/2,k,n)} - (\phi_y)_{(i,j-1/2,k,n)}\}\\ &\quad - (1/\Delta z)\{(\phi_z)_{(i,j,k+1/2,n)} - (\phi_z)_{(i,j,k-1/2,n)}\} = 0\end{aligned} \tag{23}$$

In Eq. (23), ϕ_y and ϕ_z are always calculated from a centered expression. However, the approximation of ϕ_{x^*} strongly depends on whether locally, at a point, the flow is subsonic, supersonic, sonic, or if it is a shock point. Extending the methodologies from Refs. 31 and 35 to our case, a centered approximation and a backward expression are given for u^* [defined in Eq. (21)].

$$u^{*c}_{(i,j,k,n)} = K + f(j, k, n) + (1/\gamma)g(j, k, n) + ((\gamma + 1)/2\Delta x^*)[\phi(i + 1, j, k, n) - \phi(i - 1, j, k, n)] \tag{24a}$$

$$u^{*b}_{(i,j,k,n)} = K + f(j, k, n) + (1/\gamma)g(j, k, n) + ((\gamma + 1)/2\Delta x^*)[\phi(i, j, k, n) - \phi(i - 2, j, k, n)] \tag{24b}$$

The local type of the flow is determined by Table 1 (for detailed explanations refer to Refs. 31 and 35).

Table 1 Algorithm for local type of flow

Condition	u^{*c}	u^{*b}	Local flow
1	<0	<0	subsonic
2	>0	>0	supersonic
3	>0	<0	sonic point
4	<0	>0	shock point

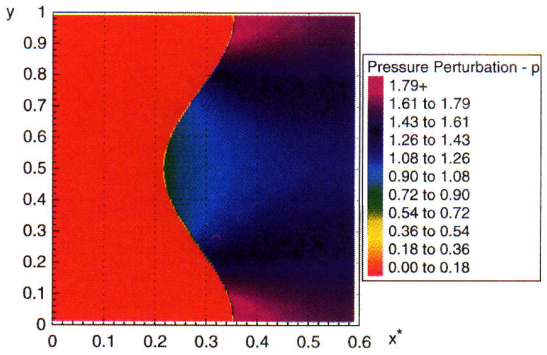

Fig. 1 Nondimensional pressure field for disturbances given by Eq. (25).

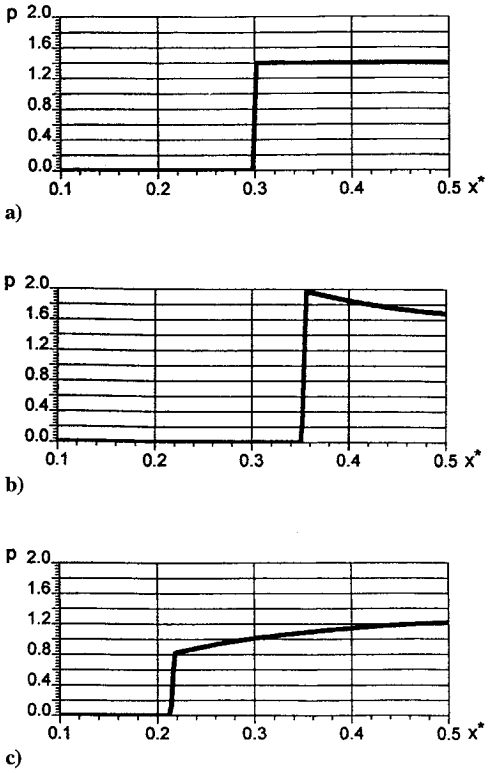

Fig. 2 Nondimensional pressure profiles at various cross sections for disturbances given by Eq. (25): a) nominal shock wave, b) at $y = 0.0$, and c) at $y = 0.5$.

Equation (23) is developed in a specific form according to the local type of the flow. When the flow is locally subsonic, an elliptic difference form is used; when the flow is locally supersonic, a hyperbolic difference form is used. A special difference form is used when the flow accelerates through the speed of sound where $(\gamma + 1)\phi_{x^*} + K + f + g/\gamma = 0$. When locally the flow passes through a shock, a special shock point difference operator is used where the flux ahead of the shock may be approximated by a backward formula and the flux behind the shock by a centered formula. A detailed description of the various difference operators is presented in Refs. 36 and 37.

Starting from initial conditions that describe a given planar shock wave for $t = 0$ and given temperature fluctuations $f(y, z, t)$ and

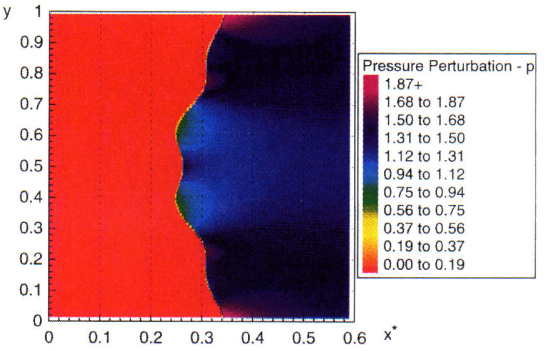

Fig. 3 Nondimensional pressure field for disturbances given by Eq. (26).

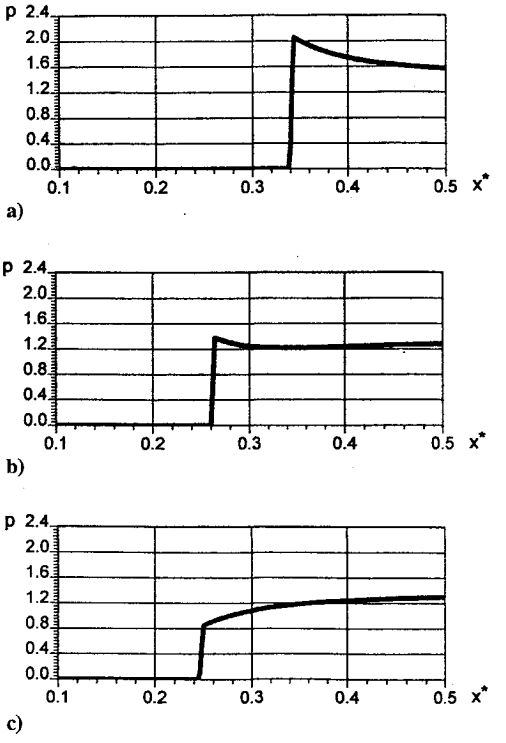

Fig. 4 Nondimensional pressure profiles at various cross sections for disturbances given by Eq. (26): a) at $y = 0.0$, b) at $y = 0.5$, and c) at $y = 0.6$.

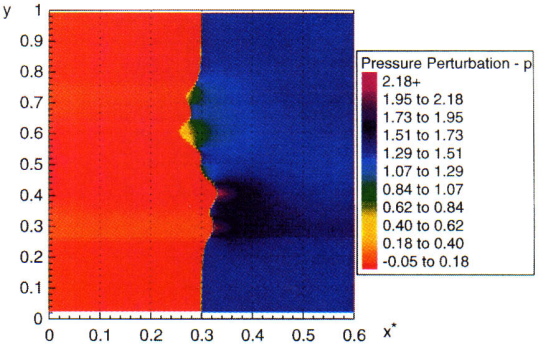

Fig. 5 Nondimensional pressure field for disturbances given by Eq. (27).

vorticity perturbations $g(y, z, t)$, the difference equations can be applied according to Table 1 and can be solved by an iterative point or line, or plane, relaxation algorithm. Convergence was determined when the residual dropped five orders of magnitude from its initial value. In this way the shock motion and pressure field behind it can be integrated in space and time and the effect of various freestream fluctuations f and g can be studied.

The present numerical scheme is formally first-order accurate, $O[\Delta x, (\Delta y)^2, (\Delta z)^2, \Delta t]$. For steady flow cases considered in

Sec. V, the numerical analysis shows second-order accuracy in the subsonic regime. The mixed-type differencing and conservative nature of the numerical formulation produces a sharp resolution of the shock wave front, spread over only three mesh points, and is independent of the mesh increment size. Both the theoretical analysis of Cole and Cook[31] and numerical studies by Giddings[37] confirm this behavior. Also presented in Ref. 37 is a variety of mesh convergence studies. As mesh is refined, the numerical accuracy of the solution is increased.

V. Numerical Results

The finite difference algorithm just outlined has been applied to a variety of two-dimensional, steady shock wave interactions with vorticity and temperature disturbances. A uniform 300 × 100 point mesh was used in all cases with $\Delta x^* = 0.002$ and $\Delta y = 0.01$. This mesh was found to give well-converged results.[37] Numerical accuracy of all pressure profiles shown here is less than 0.1%. This has been checked against calculations where more refined meshes were used. The problems considered a basic shock wave centered in the computational domain ($x = 0.3$) with the similarity parameter $K = 1.2$ and subjected to deterministic freestream fluctuations. The boundary condition $\phi_x^* = 0$ along the inlet surface was used for all cases.

The first case had periodic boundary conditions in the y direction on the $y = 0$ and $y = 1$ surfaces, whereas the downstream surface was allowed to develop freely, i.e., dictated by the upstream flow only. For this problem, the following deterministic fluctuations were used.

$$f(y) + g(y)/\gamma = 0.5\cos(2\pi y), \quad 0 \le y \le 1 \tag{25}$$

The calculated nondimensional pressure perturbation field and profiles along various cross sections are shown in Figs. 1 and 2, respectively, where Fig. 2a depicts the nominal shock solution for a flowfield without disturbances. The bending of the shocks is in phase with the velocity perturbations (Fig. 1) (i.e., a positive velocity perturbation produces a deflection in the positive y direction and vice versa) as was also described by Ribner[21] and Lee et al.[27] Relative to the nominal shock, the shock pressure jump varies along the front by about ±40% (Figs. 2b and 2c). The rippled wave front clearly leads to focusing and defocusing effects behind the shock, where diffraction effects also become significant.

To demonstrate the physical meaning of f and g functions as described in Eq. (25), let us consider a basic shock with a pressure jump of $\Delta p = p - p_\infty = 9.6 \times 10^{-4}$ bar running in a standard atmosphere where $p_\infty = 1.0132$ bar, speed of sound is $a_\infty = 340$ m/s, and temperature is $T_\infty = 288$ K. For the case where $K = 1.2$, we find from the pressure jump relation across a shock $\Delta p/p_\infty = 2\gamma(M_\infty^2 - 1)/(\gamma + 1)$, that $M_\infty = 1.0004$ and so $\epsilon^{\frac{2}{3}} = 7.10^{-4}$. Therefore, using Eqs. (11) and (18), Eqs. (25) represent, in the frame moving with the shock, either axial velocity variations in space having a similar profile with an amplitude of 0.12 m/s or temperature variations in space having a similar profile with an amplitude of 0.1 K. Both perturbations may occur in the atmosphere under regular weather conditions and will result during the passage of the basic shock in pressure jump increases or decreases of about 40%, depending on the location along the shock front.

The second case employed the same periodic boundary conditions in the y direction as in case 1. Here the disturbances were given by

$$f(y) + g(y)/\gamma = 0.3\cos(2\pi y) + 0.3\cos(4\pi y), \quad 0 \le y \le 1 \tag{26}$$

The nondimensional pressure perturbation field and profiles along various cross sections are presented as in Figs. 3 and 4, respectively. Again, the shock wave distortion results in significant local pressure jump increases and reductions (see Figs. 4a–4c). The basic effects involved are similar to those described for the first case. Note that for the steady-state case, temperature (or speed of sound) fluctuations affect the pressure fields in the same way as vorticity disturbances since they appear as a combined term $f(y) + g(y)/\gamma$ in Eq. (19c). Their relative contributions to this combined term do not influence the pressure field. Temperature and vorticity fluctuations do not, however, result in the same temperature, density, or entropy fields inasmuch as these also depend on f and g and not only the potential field. Axial velocity and temperature variations in space represented by Eq. (26) are similar to those described for the first case.

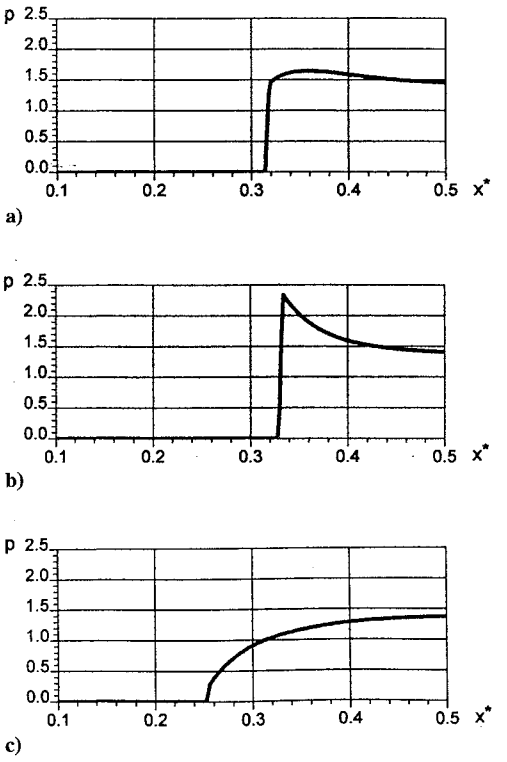

Fig. 6 Nondimensional pressure profiles at various cross sections for disturbances given by Eq. (27): a) at $y = 0.34$, b) at $y = 0.4$, and c) at $y = 0.6$.

The third case involved the following unique boundary conditions: $\phi_x^* = -1$ along the outlet surface (consistent with the nominal shock solution) and $\phi_y = 0$ along the upper and lower boundaries (as if the domain were confined by a solid boundary on the upper and lower surfaces). The disturbances in this case were given as

$$f(y) + \frac{g(y)}{\gamma} = \begin{cases} 0 & 0 \le y \le \frac{1}{4} \\ 0.5(\sin[4\pi(y - \frac{1}{4})] + \sin[16\pi(y - \frac{1}{4})]); & \frac{1}{4} \le y \le \frac{3}{4} \\ 0 & 0 \le y \le 1 \end{cases} \tag{27}$$

The numerical results are shown in Figs. 5 and 6. It was found that the shock jump was virtually eliminated in some places due to the combined effects of the disturbances. This resulted in a rounded pressure profile (Fig. 6c). At other locations along the shock front, the pressure jump across the shock is significantly increased relative to the nominal shock jump with approximately 70% (see Fig. 6b). The physical meaning of the perturbations described in Eqs. (27) is similar to those described earlier for the first case.

VI. Conclusions

The review of the theoretical studies of the interaction of shock waves with freestream vortical flows or turbulence shows that this complex nonlinear interaction is still an open problem. The analysis of the linearized problem of the interaction of a weak shock with relatively small disturbances shows that it is an invalid approach when the perturbations are of the order of shock strength. Nevertheless, in a coordinate system moving with the basic weak shock, the problem may fit the framework of transonic theory.

A new transonic small-disturbance model has been developed where a rescaling of the axial coordinate and time has been considered to capture the basic nonlinear effects that occur in the flow across the shock. This model results in two alternative approaches: 1) an equation for solving a velocity potential function that is described by an extended version of the classic small-disturbance equation for unsteady transonic aerodynamics[31] and 2) a nonlinear stochastic equation to describe the pressure field that is similar to the model equation recently presented by Pierce[17] using physical considerations only. This equation also has an extended form of the classic equation that describes the propagation of nonlinear sound beams with narrow angular spectrum.[32,33]

Both approaches show that diffraction effects, nonlinear steepening, focusing effects, and random induced freestream fluctuations interact simultaneously to determine the development of a shock wave in space and time and the pressure field behind it. Turbulence fluctuations tend to change the local speed of sound in the flow across the shock and through this effect to reduce or magnify the strength of the basic shock.

A finite difference scheme that uses Murman and Cole[35] finite-difference techniques for solving mixed-typed elliptic/hyperbolic flows with shock waves has also been presented. Numerical simulations of two-dimensional and steady shock wave iteractions with various deterministic vorticity and temperature disturbances have been shown. Results describe complicate shock wave structures and peaked, as well as rounded, local pressure signatures behind the distorted shock fronts. Similar signatures were recorded in the experiments of sonic booms running through atmospheric turbulence.[1–5] Comparison with these is difficult, however, since in all cases specific atmospheric conditions were not measured at the points where signatures were recorded.

Acknowledgments

This work was carried out with the support of the NASA Langley Research Center under Award NAG-1-1362 and NASA Training Grant NGT-S1113 and the U.S. Air Force Office of Scientific Research under Grant F49620-93-10022DEF. The authors would like to acknowledge G. L. McAninch for monitoring this research.

References

[1]Hubbard, H. H., Maglieri D. J., Huckel, V., and Hilton, D. A., "Ground Measurements of Sonic Boom Pressures for the Altitude Range of 10,000 to 75,000 Feet," NASA TR R-198, July 1964.

[2]Maglieri, D. J., "Sonic Boom Flight Research—Some Effects of Airplane Operations and the Atmosphere on Sonic Boom Signatures," *Sonic Boom Research,* edited by A.R. Seebass, NASA SP-147, April 1967.

[3]Garrick, I. E., and Maglieri, D. J., "A Summary of Results on Sonic Boom Pressure-Signature Variations Associated with Atmospheric Conditions," NASA TN D-4588, May 1968.

[4]Downing, M. J., "Lateral Spread of Sonic Boom Measurements from U.S. Air Force Boomfile Flight Tests," *High Speed Research: Sonic Boom,* edited by C. M. Darden, NASA CP-3172, Feb. 1992, pp. 117–135.

[5]Willshire, W. L., Jr., and Devilbiss, D. W., "Preliminary Results from the White Sands Missile Range Sonic Boom Propagation Experiments," *High Speed Research: Sonic Boom,* edited by C. M. Darden, NASA CP-3172, Feb. 1992, pp. 137–149.

[6]Lipkens, B., and Blackstock, T. T., "Model Experiment to Study the Effect of Turbulence on Risetime and Waveform of N Waves," *High Speed Research: Sonic Boom,* edited by C. M. Darden, NASA CP-3172, Feb. 1992, pp. 97–107.

[7]Leatherwood, J. D., and Sullivan, B. M., "Subjective Loudness Response to Simulated Sonic Booms," *High Speed Research: Sonic Boom,* edited by C. M. Darden, NASA CP-3172, Feb. 1992, pp. 151–170.

[8]Crow, S. C., "Distortion of Sonic Bangs by Atmospheric Turbulence," *Journal of Fluid Mechanics,* Vol. 37, Pt. 3, 1969, pp. 529–563.

[9]Plotkin, K. J., and George, A. R., "Propagation of Weak Shock Waves Through Turbulence," *Journal of Fluid Mechanics,* Vol. 54, Pt. 3, 1972, pp. 449–467.

[10]Ffowcs Williams, J. E., and Howe, M. S., "On the Possibility of Turbulent Thickening of Weak Shock Waves," *Journal of Fluid Mechanics,* Vol. 58, Pt. 3, 1973, pp. 461–480.

[11]Pierce, A. D., "Spikes on Sonic-boom Pressure Waveforms," *Journal of the Acoustical Society of America,* Vol. 44, No. 4, 1968, pp. 1052–1061.

[12]Pierce, A. D., "Statistical Theory of Atmospheric Turbulence Effects on Sonic-Boom Rise Times," *Journal of the Acoustical Society of America,* Vol. 49, No. 3, Pt. 2, 1971, pp. 906–924.

[13]Cramer, M. S., and Seebass, A. R., "Focusing of Weak Shock Waves at an Arête," *Journal of Fluid Mechanics,* Vol. 88, Pt. 2, 1978, pp. 209–222.

[14]Gill, M., and Seebass, A. R., "Nonlinear Acoustic Behavior at a Caustic: An Approximate Analytical Solution," AIAA Paper 73-1037, 1973.

[15]Sturtevant, B., and Kulkarny, V. A., "The Focusing of Weak Shock Waves," *Journal of Fluid Mechanics,* Vol. 73, 1976, pp. 651–671.

[16]Sparrow, V. W., and Pierce, A. D., "Simulations of Sonic Boom Ray Tube Area Fluctuations for Propagation Through Atmospheric Turbulence Including Caustics via a Monte Carlo Method," *High Speed Research: Sonic Boom,* edited by C. M. Darden, NASA CP-3172, Feb. 1992, pp. 49–62.

[17]Pierce, A. D., "Wave Equations and Computational Models for Sonic Boom Propagation Through a Turbulent Atmosphere," *High Speed Research: Sonic Boom,* edited by C. M. Darden, NASA CP-3172, Feb. 1992, pp. 31–48.

[18]Hollingsworth, M. A., and Richards, E. J., "A Schlieren Study of the Interaction Between a Vortex and a Shock Wave in a Shock Wave in a Shock Tube," British Aeronautical Research Council, Rept. 17985, FM2323, 1955.

[19]Dosanjh, D. S., and Weeks, T. M., "Interaction of a Starting Vortex as Well as a Vortex Street with a Traveling Shock Wave," *AIAA Journal,* Vol. 3, Feb. 1965, pp. 216–223.

[20]Naumann, A., and Hermanns, E., "On the Interaction Between a Shock Wave and al Vortex Field," *Noise Mechanisms,* AGARD CP-131, 1973, pp. 23-1–23-11.

[21]Ribner, H. S., "Spectra of Noise and Amplified Turbulence Emanating from Shock-Turbulence Interaction," *AIAA Journal,* Vol. 25, No. 3, 1987, p. 436.

[22]Kovasnay, L. S. G., "Turbulence in Supersonic Flow," *Journal of the Aeronautical Sciences,* Vol. 20, Oct. 1953, pp. 657–674.

[23]Moore, F. K., "Unsteady Oblique Interaction of a Shock Wave with a Plane Disturbance," NACA Rept. 1165, 1954.

[24]Ribner, H. S., "Shock-Turbulence Interaction and the Generation of Noise," NACA Rept. 1233, 1955.

[25]Chang, C. T., "Interaction of a Plane Shock and Oblique Plane Disturbances with Special Reference to Entropy Waves," *Journal of the Aeronautical Sciences,* Vol. 24, Sept. 1957, pp. 675–682.

[26]Ribner, H. S., "Cylindrical sound Wave Generated by Shock-Vortex Interaction," *AIAA Journal,* Vol. 23, No. 11, 1985, pp. 1708–1715.

[27]Lee, S., Lele, S. K., and Moin, P., "Direct Numerical Simulation of Isotropic Turbulence Interacting with a Weak Shock Wave," *Journal of Fluid Mechanics,* Vol. 251, June 1993, pp. 533–562.

[28]Zang, T. A., Hussaini, M. Y., and Bushnell, D. M., "Numerical Computations of Turbulence Amplification in Shock-Wave Interactions," *AIAA Journal,* Vol. 22, No. 1, 1984, pp. 13–21.

[29]Meadows, K. R., Kumar, A., and Hussaini, M. Y., "Computational Study on the Interaction Between a Vortex and a Shock Wave," *AIAA Journal,* Vol. 29, No. 2, 1991, pp. 174–179.

[30]Ellzey, J. L., Picone, M., and Oran, E. S., "The Interaction of a Shock with a Compressible Vortex," Naval Research Lab. M. R. 6919, 1992.

[31]Cole, J. D., and Cook, L. P., *Transonic Aerodynamics,* North-Holland, Amsterdam, 1986, pp. 46–70, 298–321.

[32]Zabolotskaya, E. A., and Khorkhlov, R. V., *Akusticheskii Zhurnal,* Vol. 15, No. 1, 1969, p. 40.

[33]Kuznetsov, V. O., *Akusticheskii Zhurnal,* Vol. 6, No. 4, 1970, p. 548.

[34]Courant, R., and Friedrichs, K. O., *Supersonic Flow and Shock Waves,* Interscience New York, 1948, pp. 297–302.

[35]Murman, E. M., and Cole, J. D., "Calculation of Plane Steady Transonic Flows," *AIAA Journal,* Vol. 9, No. 1, 1971, pp. 114–121.

[36]Rusak, Z., and Cole, J. D., "Interaction of the Sonic Boom with Atmospheric Turbulence," AIAA Paper 93-2943, July 1993.

[37]Giddings, T. E., "Interactions of Shock Waves with Vortical Flows and Turbulence," Master's Thesis, Dept. of Mechanical Engineering, Aeronautical Engineering and Mechanics, Rensselaer Polytechnic Inst., Troy, NY, Aug. 1993.